Effect of heavy-ion irradiation on London penetration depth in overdoped $Ba(Fe_{1-x}Co_x)_2As_2$

J. Murphy,[1] M. A. Tanatar,[1] Hyunsoo Kim,[1] W. Kwok,[2] U. Welp,[2] D. Graf,[3] J. S. Brooks,[3] S. L. Bud'ko,[1] P. C. Canfield,[1] and R. Prozorov[1]

[1]*Ames Laboratory and Department of Physics and Astronomy, Iowa State University, Ames, Iowa 50011, USA*

[2]*Argonne National Laboratory, Argonne, Illinois 60439, USA*

[3]*National High Magnetic Field Laboratory, Florida State University, Tallahassee, Florida 32310, USA*

(Received 2 August 2013; revised manuscript received 8 August 2013; published 27 August 2013)

Irradiation with 1.4 GeV ^{208}Pb ions was used to induce artificial disorder in single crystals of iron-arsenide superconductor $Ba(Fe_{1-x}Co_x)_2As_2$ and to study its effects on the temperature-dependent London penetration depth and transport properties. A study was undertaken on overdoped single crystals with $x = 0.108$ and $x = 0.127$ characterized by notable modulation of the superconducting gap. Irradiation corresponding to the matching fields of $B_\phi = 6$ T and 6.5 T with doses 2.22×10^{11} d/cm^2 and 2.4×10^{11} d/cm^2, respectively, suppresses the superconducting T_c by approximately 0.3 to 1 K. The variation of the low-temperature penetration depth in both pristine and irradiated samples is well described by the power law $\Delta\lambda(T) = AT^n$. Irradiation increases the magnitude of the prefactor A and decreases the exponent n, similar to the effect of irradiation in optimally-doped samples. This finding supports universal $s_\pm$ pairing in $Ba(Fe_{1-x}Co_x)_2As_2$ compounds for the entire Co doping range.

DOI: 10.1103/PhysRevB.88.054514 PACS number(s): 74.70.Dd, 72.15.−v, 68.37.−d, 61.05.cp

I. INTRODUCTION

Soon after the discovery of superconductivity in iron-based materials,[1] the strength of electron-phonon coupling in the compounds was recognized as insufficient to explain T_c in the 50 K range.[2] Together with proximity to the magnetic quantum critical point in the doping phase diagram,[3–6] this fact suggests that superconductivity in iron pnictides can be magnetically mediated, a scenario intensely discussed for cuprates, heavy fermion and organic superconductors.[7,8]

Studies of the structure of the superconducting order parameter and thus the pairing mechanism can provide important insight into the problem. For the explanation of early experiments in iron pnictides, showing both full gap[9] and neutron resonance,[10] a pairing state was suggested in which the superconducting order parameter changes sign on different Fermi surface sheets[11,12] and enables pairing by Coulomb repulsion.[13] Contrary to the d-wave state in the cuprates,[14] this so-called $s_\pm$ pairing may or may not exhibit nodes and, if it does, the nodes are accidental.[15] The full gap is indeed found at optimal doping in electron-doped NdFeAs(O,F)[9,16] and $Ba(Fe_{1-x}Co_x)_2As_2$ (BaCo122 in the following),[17,18] hole-doped $(Ba_{1-x}K_x)Fe_2As_2$ (BaK122 in the following),[19] and in stoichiometric LiFeAs.[20–22] Studies of the doping evolution of the superconducting gap in BaCo122 and in BaK122 found a nearly universal development of a strong gap anisotropy and even nodes at the dome edges.[17–19,23–26] An explanation of this evolution was suggested, considering accidental nodes in the $s_\pm$ scenario as a result of a competition between intraband Coulomb repulsion, tending to develop gap anisotropy within each band and the interband attraction[27] or as the phase transition from $s_\pm$ to a d-wave pairing state.[28] The former scenario is supported by the experimentally-determined doping evolution of the gap in overdoped BaK122,[29] whereas the latter scenario finds support in the nonmonotonic pressure dependence of T_c (Ref. 30) and the universal character of thermal conductivity.[26]

While the full isotropic superconducting gap at optimal doping is consistent with the $s_\pm$ model, this explanation is not unique. It was also discussed that orbital-mediated pairing can lead to a full gap s_{++} state.[31] In addition, theoretical calculations show the $s_\pm$, s_{++} and d-wave states are very close in energy, and the resultant ground state can depend sensibly on fine structural, magnetic, and electronic details, for example, an angle of the As-Fe-As bond.[32]

The experimental distinction between these possible pairing states is not trivial. It was suggested that T_c should be strongly sensitive to nonmagnetic impurities because of the sign change of the order parameter in $s_\pm$, similar to nodal d wave, but the two states should show different evolutions of the quasiparticle excitations. These can be revealed, for example, in the low-temperature exponents of the London penetration depth, $\Delta\lambda(T) = AT^n$ (Ref. 33). Therefore, a deliberate introduction of the additional disorder may serve as an important tuning parameter to distinguish between different superconducting states. Indeed, iron-based superconductors have some inherent amount of disorder associated with random distribution of dopant atoms required to induce superconductivity. This may explain the experimentally-observed power-law exponent n in BaCo122, which is close to two for all dopings.[34]

It was known from studies on high-T_c cuprates that extended defects, created by heavy-ion irradiation, not only act as efficient vortex pinning centers, but also as scattering sites. This is evident from a clear increase in normal state resistivity and a suppression of T_c. For iron arsenides, irradiation with heavy ions leads to a decrease of the exponent n and an increase of the prefactor A in both optimally-doped BaCo122[35] and BaK122,[36] consistent with the $s_\pm$ scenario. The change of T_c, on one hand, is still an open question and is at best moderate[35] or nondetectable.[36] On the other hand, electron irradiation results in a clear reduction of T_c in these systems, so disorder works as expected.[37,38]

In this work, we study experimentally the effect of heavy-ion irradiation in overdoped superconductors, where the superconducting gap is strongly anisotropic from the

start, even in the pristine state. Specifically, we measured London penetration depth (and thus quasiparticle excitations) in pristine and irradiated overdoped single crystals of the BaCo122 family. These compositions are characterized by a strong gap anisotropy as found in temperature and magnetic field response of thermal conductivity.[17,18] The selection of these materials was motivated by the fact that in s_{++} superconductors with accidental nodes, the disorder should wipe out gap minima. Therefore, its effect should be very different from that for the $s_{\pm}$ state. Additionally, we studied resistivity in various magnetic fields and determined the upper critical field H_{c2} to test a recently suggested link between the anisotropy of the gap and T-linear $H_{c2,c}(T)$ in $H\|c$ configuration.[39,40]

II. EXPERIMENTAL

A. Sample preparation

Single crystals of $BaFe_2As_2$ were grown from FeAs flux and doped with Co from a starting load of elemental Ba, FeAs, and CoAs, as described in detail elsewhere.[41] Crystals were thick platelets with sizes as big as $12 \times 8 \times 1$ mm^3 and large faces corresponding to the tetragonal (001) plane. The actual content of Co in the crystals was determined with wavelength dispersive electron probe microanalysis and is the x value used throughout this text. The two compositions studied were $x = 0.108$ ($T_c \approx 16$ K) and $x = 0.127$ ($T_c \approx 8$ K) from the same batches used in previous thermal conductivity studies.[17,18] They were on the overdoped side of the doping phase diagram (see inset in Fig. 1), notably above the optimal doping level $x_{\rm opt} = 0.07$ ($T_c \approx 23$ K).

B. Measurements of London penetration depth

The in-plane London penetration depth was measured using the tunnel diode resonator (TDR) technique.[42] The sample was mounted on a sapphire rod inserted into the inductor coil (L) component of an LC Tank circuit, creating ac magnetic field, $H_{ac} \sim 20$ mOe. Since $H_{ac} \ll H_{c1}$, the sample remains in the Meissner state and the magnetic response is governed by the London penetration depth. During the experiments, H_{ac} was parallel to the sample c axis, thus measuring field penetration along the conducting plane. The presence of the sample in the coil causes a frequency shift, which can be related to the change in the inductance of the TDR circuit $\Delta f = f_0 - f(T)$, where $f_0 = 1/(2\pi\sqrt{LC}) \sim 14$ MHz. The real part of the magnetic susceptibility χ(T) can then be derived, $\Delta f = -G4\pi\chi(T)$. The calibration factor, $G = f_0 V_s/[2V_c(1-N)]$, is defined by the sample volume V_s, coil volume V_c, and the demagnetization factor N. Experimentally, G is directly measured by physically pulling the sample from the coil *in situ* at low temperatures. With the sample in the Meissner state, λ can be obtained from the following relation: $4\pi\chi(T) = \lambda/R \tanh(R/\lambda) - 1$, where R is the effective dimension of the sample.[43]

To measure the changes in the superconducting transition temperature, T_c, and the change in the penetration depth, $\Delta\lambda(T)$, with irradiation, the same samples were first measured using a TDR setup in a ^{3}He cryostat (to 0.5 K) and then in a dilution refrigerator to 0.05 K.[44] Reference samples were stored in the same environment as irradiated samples and re-measured to assure no degradation during storage. They were used in the upper critical field measurements afterwards, with contacts soldered for resistivity measurements.

C. Heavy ion irradiation

To create columnar defects, the samples were irradiated with 1.4 GeV ^{208}Pb ions at the Argonne Tandem Linear Accelerator System (ATLAS). The ions at this energy have a stoppage distance of about 70 μm, so, prior to irradiation, all samples were cleaved to a thickness of 30 μm or less to ensure a homogeneous effect of irradiation. The flux and the dose of irradiation were measured during each irradiation experiment. The irradiation dose was 2.22×10^{11} d/cm^2 for the $x = 0.127$ sample and 2.4×10^{11} d/cm^2 for the $x = 0.108$ sample. Traditionally, the density of columnar defects d is characterized using a matching magnetic field $B_\phi = \Phi_0 d$, calculated by assuming one magnetic flux quantum, $\Phi_0 \approx 2.07 \times 10^{-7}$ G cm^2, per ion track. The samples studied here where given 6 and 6.5 T equivalent doses.

D. Electrical resistivity and upper critical field measurements

In-plane electrical resistivity ρ and the upper critical field measurements were performed on reference samples cut from the same crystals used in the penetration depth study. Samples were cleaved into a rectangular shape with the crystallographic a axis along the long side. Contacts were made by soldering silver wires with ultrapure tin,[45,46] resulting in a very low contact resistance (less than 10 $\mu\Omega$). Resistivity measurements were made using the standard four-probe technique. Samples were initially characterized using a *Quantum Design PPMS*. The temperature-dependent resistivity of these samples is shown in the main panel of Fig. 1.

To enable measurements in high magnetic fields and to prevent sample motion during in-field rotation, the samples were glued with GE varnish to a G-10 sample stage. Sample resistance was checked after mounting and determined to agree with the measurements in a free-standing state. The stage was fitted into a single-axis rotator of a 35 T DC magnet at the National High Magnetic Field Laboratory in Tallahassee, Florida. The rotator allows over a 90° rotation around its horizontal axis in the vertical magnetic field. Measurements were made in a ^{4}He cryostat with a variable temperature insert (VTI) with lowest temperatures to 1.5 K. The presence of He gas provides a good heat link between samples on the G-10 stage and thermometer. The rotator was equipped with a stepper motor with an angular resolution of 0.01°. The magnetic field was aligned parallel to the sample plane, $\theta = 0$, using angle-dependent resistivity in a magnetic field slightly below $H_{c2,ab}$, see Ref. 48 for further details.

After finishing the penetration depth study, four contacts were soldered[45,46] to the sample with $x = 0.127$, and the temperature-dependent resistivity $\rho(T)$ was measured, see Fig. 1. Contact soldering was made at $T \sim 500$ K, which could lead to a partial annealing of irradiation damage. Note, the difference between pristine and irradiated samples for

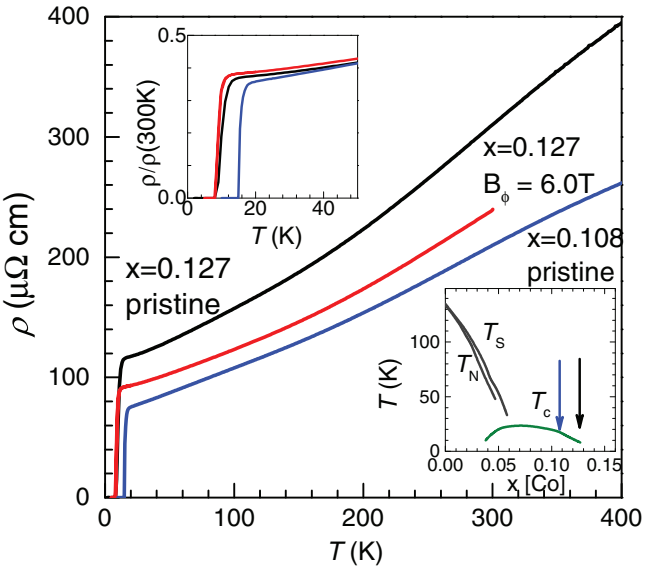

FIG. 1. (Color online) Temperature-dependent electrical resistivity for the reference samples $x = 0.108$ and $x = 0.127$, and the irradiated sample of $x = 0.127$. The irradiated sample $x = 0.127$ is the same sample as used in penetration depth measurements, with contacts soldered after measurements completed. The top inset shows the same curves using a normalized resistivity scale $\rho/\rho(300\ \mathrm{K})$, showing the main difference between resistivity values comes from the error of geometric factor determination.[41,47] The bottom inset shows a sketch of the doping phase diagram for BaCo122 with the position of the samples used in this study.

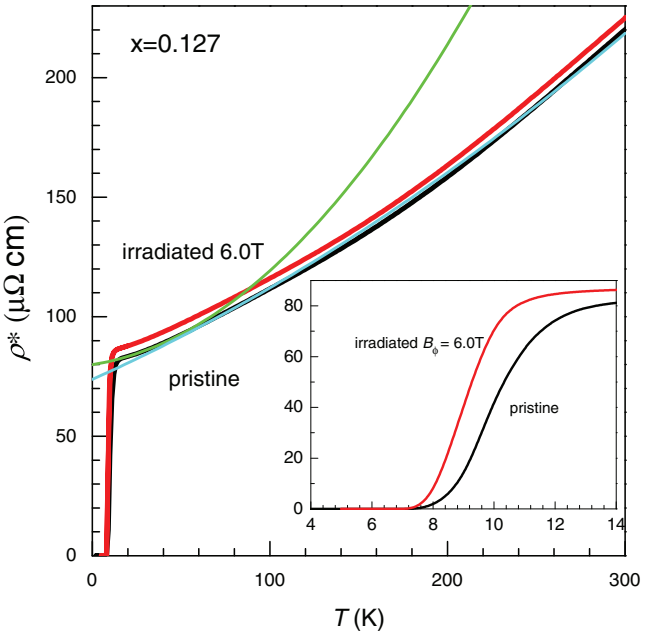

FIG. 2. (Color online) Comparison of the temperature-dependent electrical resistivity of reference and irradiated samples $x = 0.127$, with a geometric factor correction by normalizing slopes of the $\rho(T)$ curves at 300 K. For the pristine sample, we assumed $\rho(300\ \mathrm{K}) = 220\ \mu\Omega$ cm.[49] Inset zooms for the superconducting transition range. Heavy ion irradiation does not change the shape of the $\rho(T)$ curves, but increases residual resistivity, sharpens the superconducting transition, and shifts T_c downward.

$x = 0.127$ in Fig. 1 mainly comes from the error in the geometric factor determination, particularly big in micaceous crystals of iron pnictides, due to hidden cracks.[41,47] We failed to make contacts to a much thinner irradiated sample, $x = 0.108$.

III. RESULTS AND DISCUSSION

A. Resistivity change with irradiation

The $\rho(T)$ of the irradiated sample, Fig. 1, is nearly the same within uncertainty of the geometric factor with that for the reference sample.[41,47] A rough way of removing this uncertainty is to normalize the resistivity by its value at room temperature, $\rho(300\ \mathrm{K})$, as shown in the top inset in Fig. 1. This reveals that the irradiated sample has a higher normalized resistivity value at T_c and slightly lower T_c, as expected. To make a more careful $\rho(T)$ comparison, we normalized the slopes of $\rho(T)$ curves at 300 K. For the pristine sample, we also used the value of the resistivity at room temperature, $\rho(300\ \mathrm{K}) = 220\ \mu\Omega$ cm, as determined by statistically significant measurements on a large array of samples.[49] In Fig. 2, we compare temperature dependence of the adjusted resistivity, $\rho^\star(T)$, for pristine and irradiated samples with $x = 0.127$. For the pristine sample, we also show a fit of the $\rho(T)$ curve above superconducting transition using a second order polynomial, $\rho(T) = \rho_0 + \alpha T + AT^2$. This function was used to determine residual resistivity of the samples, ρ_0. The value of residual resistivity $\rho(0)$ depends slightly on the fitting range. The fit over a small range above T_c, green curve in Fig. 2, closely follows the data and gives $\rho(0) = 80\ \mu\Omega$ cm. The fit over the entire range from T_c to room temperature, cyan curve in Fig. 2, goes significantly below the actual data above T_c and gives $\rho(0) = 73\ \mu\Omega$ cm.

Heavy ion irradiation has three effects on the $\rho^\star(T)$ of the samples. (i) Irradiation slightly parallel-up-shifts the $\rho(T)$ curve, as expected for samples with increased residual resistivity obeying Matthiessen's rule. This shift allows us to quantify an additional increase of residual resistivity, due to irradiation damage as $\Delta\rho^\star(0) = 4\ \mu\Omega$ cm. This increase is significantly smaller than the extrapolated residual resistivity, $\rho(0) \approx 80\ \mu\Omega$ cm. The very small increase of the scattering rate induced by irradiation can explain the very small shift of the superconducting T_c in heavy-ion irradiated samples, provided a substitution disorder accompanying Co-doping acts for pairbreaking. (ii) Irradiation sharpens the resistive transition, which is presumably a reflection of the increased pinning on columnar defects, suppressing Kosterlits-Thouless vortex fluctuations, and breaking weak links in the samples.[50] (iii) Irradiation shifts the onset and the midpoint T_c of the superconducting transition by almost 1 K. This value is somewhat higher than that found in the penetration depth measurements, see Fig. 8 below. However, because of the transition sharpening, T_c strongly depends on the criterion used. Observation of the comparable T_c shift suggests the short-time heat treatment at ~500 K during contact soldering does not lead to a significant annealing of the defects induced by the heavy ion irradiation.

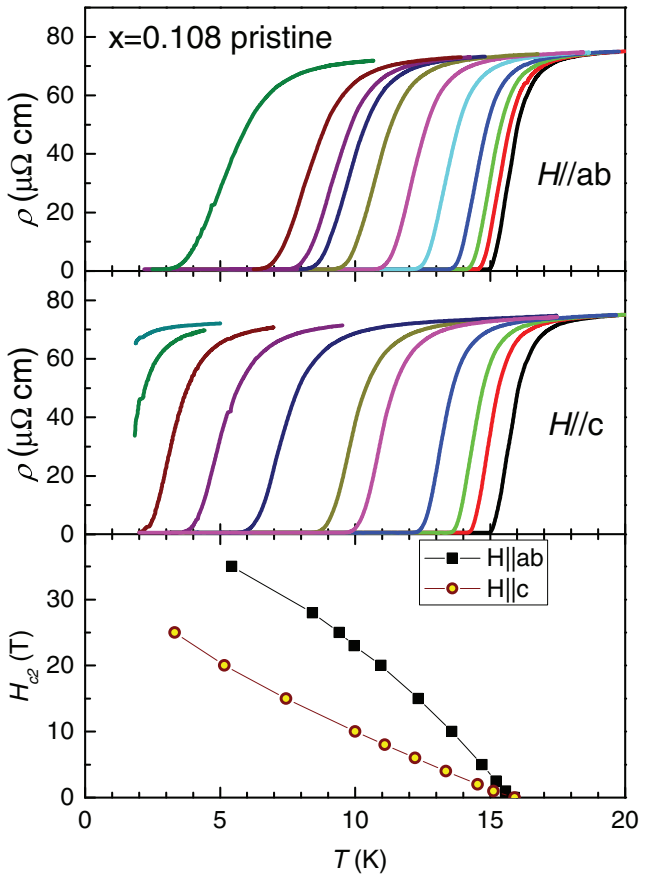

FIG. 3. (Color online) In-plane resistivity $\rho(T)$ for slightly overdoped $Ba(Fe_{1-x}Co_x)_2As_2$, $x = 0.108$, in magnetic fields (a) parallel to the conducting plane, perpendicular to the c axis, and (b) parallel to the crystallographic c axis. The field values are (right to left) 0, 1, 2.5, 5, 10, 15, 20, 23, 25, 28, and 35 T. The bottom panel (c) shows H_{c2}(T) phase diagrams for both directions of the magnetic field.

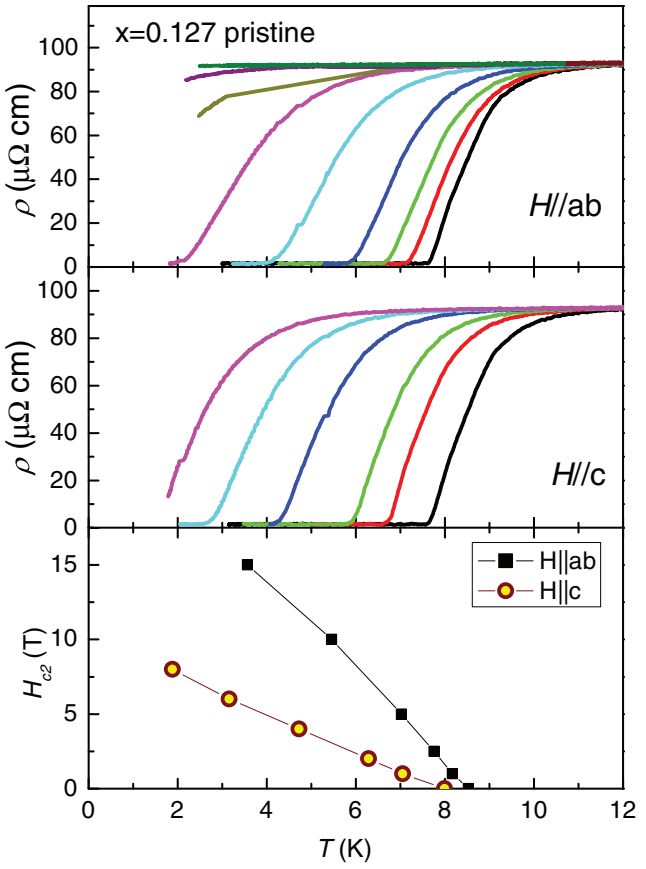

FIG. 4. (Color online) In-plane resistivity $\rho(T)$ for heavily overdoped $Ba(Fe_{1-x}Co_x)_2As_2$, $x = 0.127$ in magnetic fields (a) parallel to the conducting plane and perpendicular to the c axis, field values (right to left) 0, 1, 2.5, 5, 10, 15, 20, 23, and 25 T, and (b) parallel to the crystallographic c axis, field values (right to left) 0, 1, 2, 4, 6, 8, and 10 T. Bottom panel (c) shows H_{c2}(T) phase diagrams for both directions of magnetic field.

B. Doping evolution of the temperature dependent $H_{c2}(T)$

Recently, we reported that the shape of the temperature-dependent upper critical field for field orientation parallel to the tetragonal c axis, $H_{c2,c}(T)$, is very different for iron-arsenide superconductors with full superconducting gaps (e.g., LiFeAs[51]), and with a nodal gap [e.g., $SrFe_2(As_{1-x}P_x)_2$[39,52] and KFe_2As_2[40]]. The former shows a clear saturation at low temperatures, in line with expectations of both orbital WHH theory[53] and paramagnetic Clogston-Chandrasekhar limit,[54] while the latter remains close to T linear down to the lowest temperatures. Moreover, for KFe_2As_2, the low-temperature $H_{c2,c}(0)$ scales with T_c, which is not expected for standard orbital limiting mechanism in the clean limit.[40,55]

To gain further insight into these unusual features, we studied anisotropic upper critical fields in overdoped BaCo122 compositions, where the superconducting gap anisotropy increases towards the superconducting dome edge. We used resistive H_{c2} determination in the constant-field temperature-sweep measurements, as shown in Figs. 3 and 4, for pristine samples of BaCo122 with $x = 0.108$ and $x = 0.127$, respectively, for field orientations parallel to the conducting ab plane (top panels) and parallel to the tetragonal c axis (bottom panels). A midpoint of the resistive transition was used as a criterion to determine $H_{c2}(T)$. The bottom panels show H-T phase diagrams determined from these measurements.

In Fig. 5, we compare the results of our measurements with the results of the previous study[41] on samples $x = 0.102$ and $x = 0.114$. The two sets are in good agreement and reveal a very monotonic evolution of H_{c2} with doping. The bottom panel in Fig. 5 shows temperature-dependent anisotropy, $\gamma \equiv H_{c2,ab}/H_{c2,c}$, for samples with $x = 0.108$ and $x = 0.127$. Close to T_c the anisotropy is maximum, $\gamma = 2.5 \pm 0.5$ for $x = 0.108$ and $\gamma = 3.5 \pm 0.5$ for $x = 0.127$, with error bars determined by the difference in the criteria of resistive transition temperature determination. These values are consistent with the values found for the overdoped compositions in the previous study and significantly different from much smaller anisotropies, $\gamma \sim 1$, found in the underdoped compositions.[41]

Our $H_{c2}(T)$ measurements for the configuration with $H \| c$ for the most overdoped sample $x = 0.127$ do not extend to sufficiently low temperatures. However, the bulk thermal conductivity measurements by Reid *et al.*,[18] made on the samples

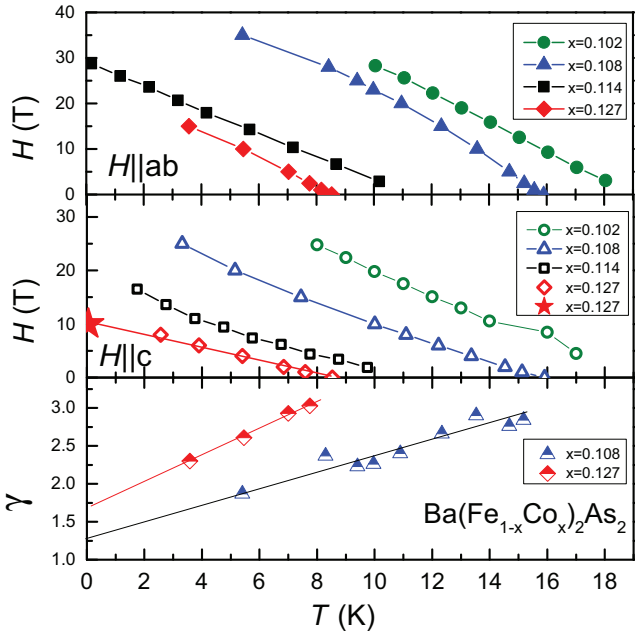

FIG. 5. (Color online) $H_{c2}(T)$ and anisotropy parameter, $\gamma \equiv H_{c2,ab}/H_{c2,c}$, for overdoped samples of BaCo122 $x = 0.108$ and $x = 0.127$. Top panel shows configurations with magnetic fields parallel to the conducting plane. The middle panel shows configurations with the magnetic field parallel to the crystallographic c axis. For reference, we show bulk $H_{c2,c}(0)$ as determined from the thermal conductivity study in the sample $x = 0.127$ (red star, Ref. 18), which suggests the data for strongly overdoped samples $x = 0.127$ show very close to T-linear dependence. The top and middle panels show data for previously studied overdoped samples with $x = 0.102$ and $x = 0.114$,[41] determined using the same midpoint criterion. The bottom panel shows the temperature-dependent anisotropy parameter for samples $x = 0.108$ and $x = 0.127$.

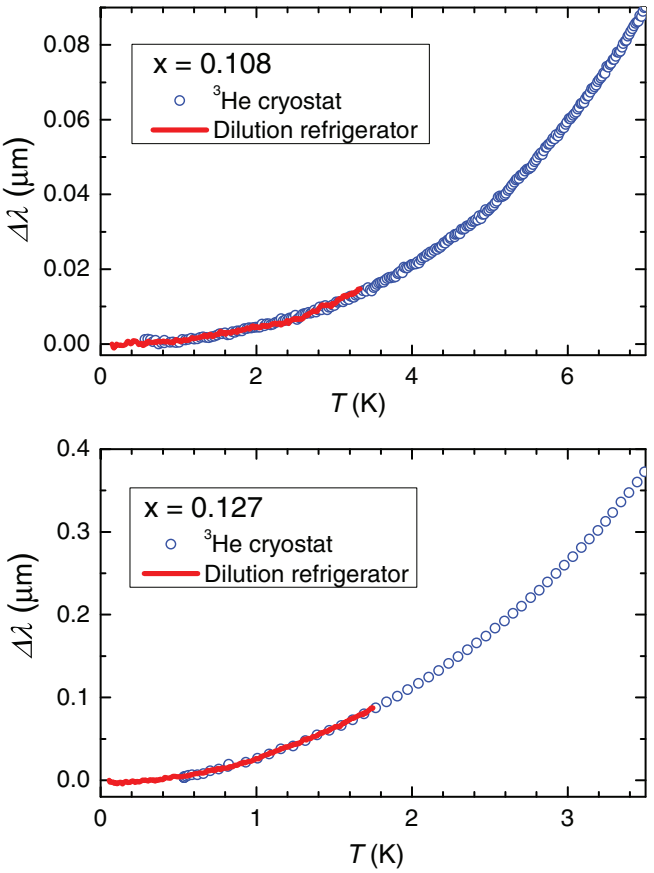

FIG. 6. (Color online) Low temperature London penetration depth $\Delta\lambda$(T) for samples of $Ba(Fe_{1-x}Co_x)_2As_2$ with $x = 0.108$ (top panel) and $x = 0.127$ (bottom panel). Data were taken in both a ^{3}He-cryostat (down to ~0.5 K, black curves) and a dilution refrigerator (~0.05 K $< T <$ 3 K, red curve), showing a good match between the data sets taken in these two systems and the robustness of the power-law dependence.

from the same batch, suggest $H_{c2,c}(0) = 10$ T, as shown by a star in the middle panel of Fig. 5. Compilations of the high temperature data from our study and the low-temperature thermal conductivity data suggest the linear $H_{c2,c}(T)$ trend is observed in $x = 0.127$, in which the superconducting gap characterized by the presence of nodes. For the sample with $x = 0.108$, we estimate $H_{c2,c}(0) \approx 30$ T.

C. London penetration depth

Figure 6 shows the temperature-dependent variation of the London penetration depth in pristine samples of BaCo122 with $x = 0.108$ (top panel) and $x = 0.127$ (bottom panel). Due to a rather low T_c (≈8 K) of the sample with $x = 0.127$, the measurements to ~0.5 K, the base temperature in our ^{3}He setup, do not cover a sufficiently broad temperature range to provide a reliable power-law analysis. We extended the temperature range by collecting the data in a dilution refrigerator to ~0.05 K or $T_c/160$. The data sets taken in two systems perfectly matched the overlapping range 0.5 to 3.5 K, providing support for the reliability of the measurements. It is clear from an inspection of the raw data, the temperature variation of the London penetration depth is stronger than the exponential variation expected in full-gap superconductors. In fact, the dependence is close to T^2, as shown in Fig. 7, where the data for two compositions are plotted vs $(T/T_c)^2$. This is similar to the earlier data by Gordon *et al.*[34] As seen from Fig. 7, the exponent n is larger for the sample with x closer to the optimal doping composition. Using a power-law fit over a temperature range to $T_c/3$, we obtain $n = 2.5$ for the sample with $x = 0.108$ and $n = 2.0$ for $x = 0.127$. These values and their changes with doping follow the general trend in iron pnictides.[56] In BaCo122 this evolution is in line with the results of thermal conductivity[17,18] and heat capacity[57] studies.

Figure 8 shows the London penetration depth from the base temperature to $\sim T_c/3$ in the sample $x = 0.108$ (top panel) before (black curve) and after 6.5 T irradiation (red curve). The inset shows the data for the entire temperature range, revealing a small, but clear, decrease of T_c. Irradiation significantly increases the total $\Delta\lambda(T)$ change from the base temperature to $T_c/3$. Similar data for the sample $x = 0.127$ in pristine (black line) and 6 T irradiated (red line) states are shown in the bottom panel of Fig. 8. The T_c decrease in the sample $x = 0.127$ is larger than for sample $x = 0.108$. Similarly, an overall change in the penetration depth to $T_c/3$ is larger as well.

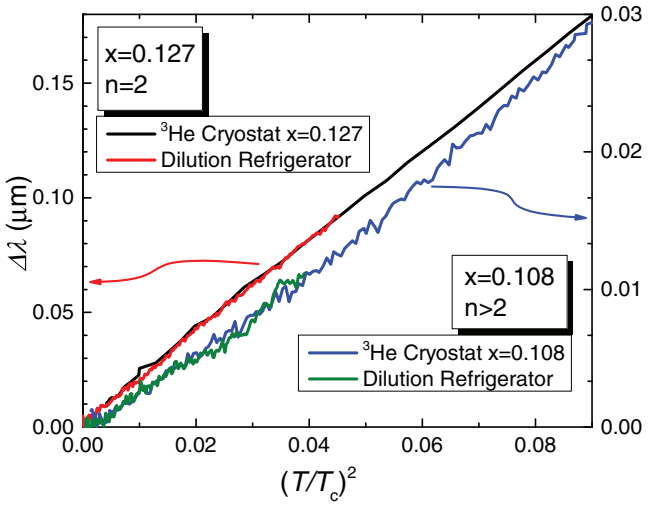

FIG. 7. (Color online) Low temperature London penetration depth $\Delta\lambda$(T) measured in single crystals of $Ba(Fe_{1-x}Co_x)_2As_2$ with $x = 0.108$ (green and blue curves) and $x = 0.127$ (black and red curves) plotted vs $(T/T_c)^2$. Linear plot for $x = 0.127$ shows the dependence is very close to T^2, consistent with more detailed fitting analysis using a floating fitting range, see Fig. 9. Clear deviations for sample $x = 0.108$ suggest $n > 2$.

In a standard analysis of the penetration depth in single gap superconductors, the low-temperature asymptotic behavior is expected in the range from the base temperature to roughly $T_c/3$, over the temperature range where the superconducting gap can be considered as constant. This assumption is invalid for multiband superconductors, in which case the high-temperature end of the fitting is determined by the smaller gap.[58] Since this ratio is *a priori* unknown, we varied the high-temperature range of the fit. We used a power-law function $\Delta\lambda(T) = AT^n$, and determined n and A as a function of the high-temperature end of the fitting range, always beginning the fit at the base temperature. The results of this fitting analysis for pristine and irradiated samples are shown in Fig. 9 for samples with $x = 0.108$ (left column) and $x = 0.127$ (right column). The top panels show the evolution of the exponent n and the bottom panels show the evolution of the prefactor A. The results of the fitting analysis, Fig. 9, indicate that for the sample with $x = 0.108$, exponent n weakly depends on the fitting range, changing from 2.7 to 2.6. In the irradiated samples the exponent decreases to $n = 2.2$ for $T_c/4.5$, and slightly increases to 2.3 for $T_c/3$. The decrease of the exponent with irradiation is not expected in either s_{++} or d-wave states, but predicted for the $s_\pm$ pairing. The effect of irradiation is even more dramatic in a sample with $x = 0.127$. Here, the exponent in the pristine sample is $n = 2.0$, a value possible to explain in both dirty d-wave and dirty $s_\pm$ scenarios.[59,60] For the former, the exponent is expected to be insensitive to the increase of scattering; for the latter, it is expected to decrease further to about 1.6. As can be clearly seen, irradiation decreases n to 1.8, suggesting an increase of anisotropy. Simultaneously, the prefactor for these samples also increases after irradiation, clearly showing the appearance of excess quasiparticles, due to additional in-gap density of states induced by pair-breaking scattering.

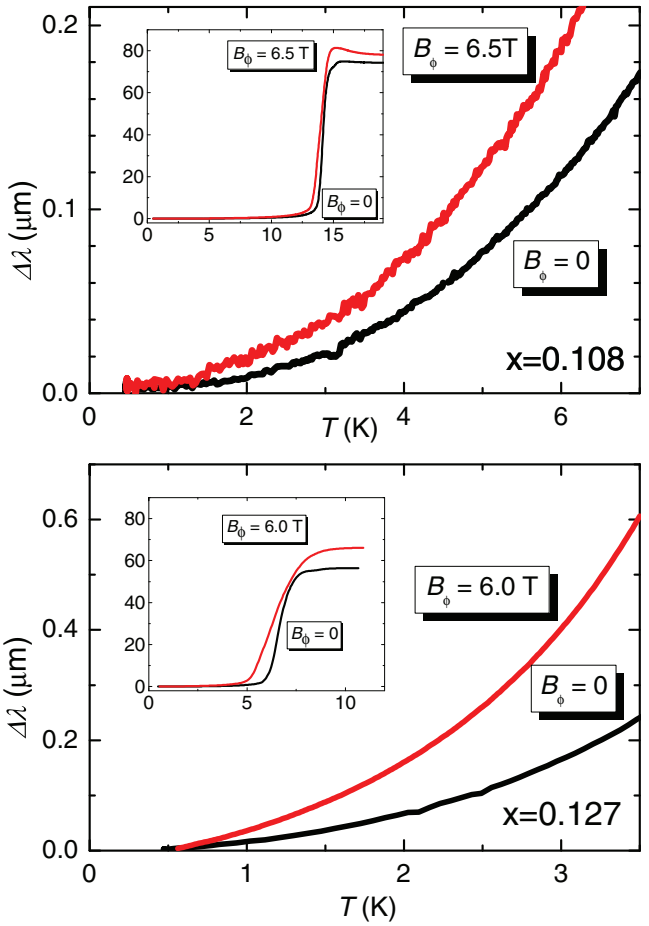

FIG. 8. (Color online) Effect of heavy-ion irradiation on London penetration depth, $\Delta\lambda(T)$ in samples with $x = 0.108$ (top) and $x = 0.127$ (bottom). Black curves show pristine samples, red curves show irradiated with matching fields of 6.5 T and 6 T, respectively. Insets show the variation of the London penetration depth in the entire range to T_c.

IV. CONCLUSIONS

In conclusion, we find the temperature-dependent London penetration depth in overdoped samples of BaCo122 is the best fit with the power law with the exponent n decreasing with x towards the overdoped edge of the superconducting dome, confirming increasing gap anisotropy. The exponent n also decreases after heavy-ion irradiation, introducing additional scattering. This observation is in line with the expectations for the $s_\pm$ pairing state with accidental nodes, but contradicts those for the s_{++} state. This suggests the $s_\pm$ pairing state is universal over the entire doping range in electron-doped BaCo122.

Considering our resistively measured $H_{c2,c}(T)$ together with the results of the previous thermal conductivity studies, we find the $H_{c2,c}(T)$ dependence in sample $x = 0.127$ at the very dome edge with nodes in the superconducting gap is very close to T linear. This observation is in line with our finding of the link between the superconducting gap anisotropy and the anomalous T-linear dependence of $H_{c2,c}$. This suggests the feature may be universal in iron-arsenide superconductors.

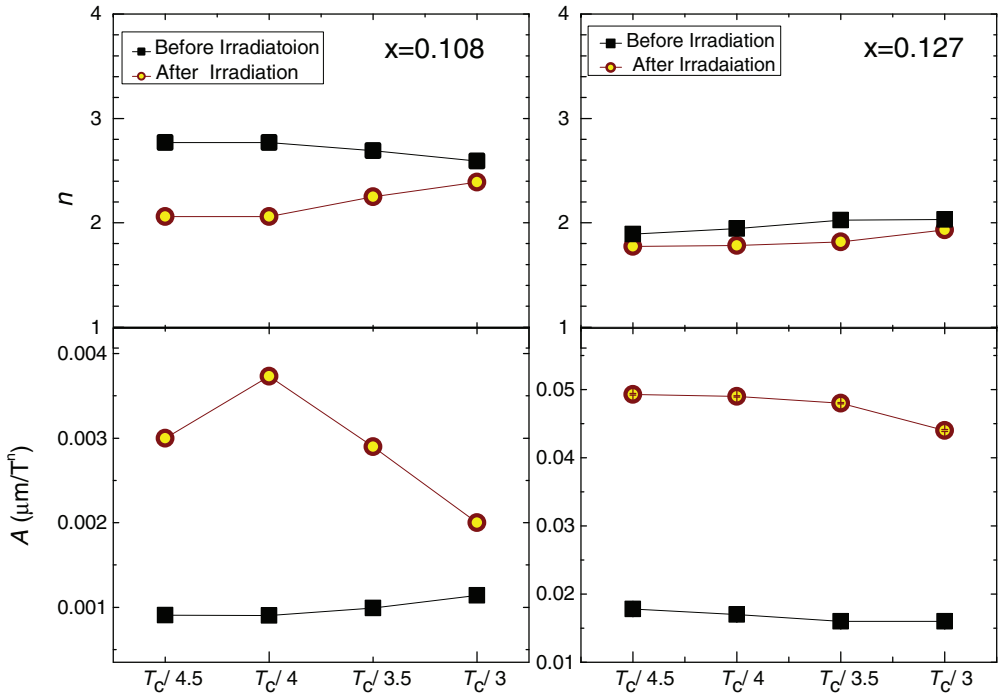

FIG. 9. (Color online) Dependence of the fitting parameters, n (top panels) and A (bottom panels), of the power-law function, $\Delta\lambda = AT^n$, on the temperature of the high-temperature boundary of the fitting interval. Data are shown for pristine (black squares) and irradiated (yellow-brown circles) sample with $x = 0.108$ (left) and $x = 0.127$ (right).

ACKNOWLEDGMENTS

Work at Ames Laboratory was supported by the US Department of Energy, Office of Basic Energy Sciences, Division of Materials Sciences and Engineering under Contract No. DE-AC02-07CH11358. Work at Argonne was supported by the Center for Emergent Superconductivity, an Energy Frontier Research Center funded by the US Department of Energy, Office of Science, Office of Basic Energy Sciences under Award No. DE-AC0298CH1088. Work at the National High Magnetic Field Laboratory is supported by the NSF Cooperative Agreement No. DMR0654118 and by the state of Florida. We thank Rebecca A. Shivvers for careful reading of the manuscript.

[1] Y. Kamihara, T. Watanabe, M. Hirano, and H. Hosono, J. Am. Chem. Soc. **130**, 3296 (2008).

[2] L. Boeri, O. V. Dolgov, and A. A. Golubov, Phys. Rev. Lett. **101**, 026403 (2008).

[3] J. Paglione and R. L. Greene, Nat. Phys. **6**, 645 (2010).

[4] D. C. Johnston, Adv. Physics. **59**, 803 (2010).

[5] P. C. Canfield and S. L. Bud'ko, Ann. Rev. Cond. Mat. Phys. **1**, 27 (2010).

[6] G. R. Stewart, Rev. Mod. Phys. **83**, 1589 (2011).

[7] P. Monthoux, D. Pines, and G. G. Lonzarich, Nature (London) **450**, 1177 (2007).

[8] M. R. Norman, Science **332**, 196 (2011).

[9] T. Y. Chen, Z. Tesanovic, R. H. Liu, X. H. Chen, and C. L. Chien, Nature (London) **453**, 1224 (2008).

[10] A. D. Christianson, E. A. Goremychkin, R. Osborn, S. Rosenkranz, M. D. Lumsden, C. D. Malliakas, I. S. Todorov, H. Claus, D. Y. Chung, M. G. Kanatzidis, R. I. Bewley, and T. Guidi, Nature (London) **456**, 930 (2008).

[11] I. I. Mazin, D. J. Singh, M. D. Johannes, and M. H. Du, Phys. Rev. Lett. **101**, 057003 (2008).

[12] Igor I. Mazin, Nature (London) **464**, 183 (2010).

[13] D. J. Scalapino, Rev. Mod. Phys. **84**, 1383 (2012).

[14] C. C. Tsuei and J. R. Kirtley, Rev. Mod. Phys. **72**, 969 (2000).

[15] P. J. Hirschfeld, M. M. Korshunov, and I. I. Mazin, Rep. Prog. Phys. **74**, 124508 (2011).

[16] Takeshi Kondo, A. F. Santander-Syro, O. Copie, Chang Liu, M. E. Tillman, E. D. Mun, J. Schmalian, S. L. Bud'ko, M. A. Tanatar, P. C. Canfield, and A. Kaminski, Phys. Rev. Lett. **101**, 147003 (2008).

[17] M. A. Tanatar, J.-Ph. Reid, X. G. Luo, H. Shakeripour, N. Doiron-Leyraud, N. Ni, S. L. Bud'ko, P. C. Canfield, R. Prozorov, and Louis Taillefer, Phys. Rev. Lett. **104**, 067002 (2010).

[18] J.-Ph. Reid, M. A. Tanatar, X. G. Luo, H. Shakeripour, N. Doiron-Leyraud, N. Ni, S. L. Bud'ko, P. C. Canfield, R. Prozorov, and L. Taillefer, Phys. Rev. B **82**, 064501 (2010).

[19] J.-Ph. Reid, A. Juneau-Fecteau, R. T. Gordon, S. Rene de Cotret, N. Doiron-Leyraud, X. G. Luo, H. Shakeripour, J. Chang, M. A. Tanatar, H. Kim, R. Prozorov, T. Saito, H. Fukazawa, Y. Kohori, K. Kihou, C. H. Lee, A. Iyo, H. Eisaki, B. Shen, H.-H. Wen, Louis Taillefer, Supercond. Sci. Technol. **25**, 084013 (2012).

[20] H. Kim, M. A. Tanatar, Yoo Jang Song, Yong Seung Kwon, and R. Prozorov, Phys. Rev. B **83**, 100502 (2011).

[21] S. V. Borisenko, V. B. Zabolotnyy, D. V. Evtushinsky, T. K. Kim, I. V. Morozov, A. N. Yaresko, A. A. Kordyuk, G. Behr, A. Vasiliev, R. Follath, and B. Buchner, Phys. Rev. Lett. **105**, 067002 (2010).

[22] M. A. Tanatar, J.-Ph. Reid, S. René de Cotret, N. Doiron-Leyraud, F. Laliberté, E. Hassinger, J. Chang, H. Kim, K. Cho, Yoo Jang Song, Yong Seung Kwon, R. Prozorov, and Louis Taillefer, Phys. Rev. B **84**, 054507 (2011).

[23] H. Fukazawa, Y. Yamada, K. Kondo, T. Saito, Y. Kohori, K. Kuga, Y. Matsumoto, S. Nakatsuji, H. Kito, P. M. Shirage, K. Kihou, N. Takeshita, C.-H. Lee, A. Iyo, and H. Eisaki, J. Phys. Soc. Jpn. **78**, 083712 (2009).

[24] J. K. Dong, S. Y. Zhou, T. Y. Guan, H. Zhang, Y. F. Dai, X. Qiu, X. F. Wang, Y. He, X. H. Chen, and S. Y. Li, Phys. Rev. Lett. **104**, 087005 (2010).

[25] K. Hashimoto, A. Serafin, S. Tonegawa, R. Katsumata, R. Okazaki, T. Saito, H. Fukazawa, Y. Kohori, and K. Kihou, C. H. Lee, A. Iyo, H. Eisaki, H. Ikeda, Y. Matsuda, A. Carrington, and T. Shibauchi, Phys. Rev. B **82**, 014526 (2010).

[26] J.-Ph. Reid, M. A. Tanatar, A. Juneau-Fecteau, R. T. Gordon, S. René de Cotret, N. Doiron-Leyraud, T. Saito, H. Fukazawa, Y. Kohori, K. Kihou, C. H. Lee, A. Iyo, H. Eisaki, R. Prozorov, and Louis Taillefer, Phys. Rev. Lett. **109**, 087001 (2012).

[27] S. Maiti, M. M. Korshunov, T. A. Maier, P. J. Hirschfeld, and A. V. Chubukov, Phys. Rev. B **84**, 224505 (2011).

[28] Ronny Thomale, Christian Platt, Werner Hanke, Jiangping Hu, and B. Andrei Bernevig, Phys. Rev. Lett. **107**, 117001 (2011).

[29] K. Okazaki, Y. Ota, Y. Kotani, W. Malaeb, Y. Ishida, T. Shimojima, T. Kiss, S. Watanabe, C.-T. Chen, K. Kihou, C. H. Lee, A. Iyo, H. Eisaki, T. Saito, H. Fukazawa, Y. Kohori, K. Hashimoto, T. Shibauchi, Y. Matsuda, H. Ikeda, H. Miyahara, R. Arita, A. Chainani, and S. Shin, Science **337**, 1314 (2012).

[30] F. F. Tafti, A. Juneau-Fecteau, M.-E. Delage, S. Rene de Cotret, J.-Ph. Reid, A. F. Wang, X.-G. Luo, X. H. Chen, N. Doiron-Leyraud, and Louis Taillefer, Nat. Phys. **9**, 349 (2013).

[31] Hiroshi Kontani and Seiichiro Onari, Phys. Rev. Lett. **104**, 157001 (2010).

[32] Kazuhiko Kuroki, Hidetomo Usui, Seiichiro Onari, Ryotaro Arita, and Hideo Aoki, Phys. Rev. B **79**, 224511 (2009).

[33] Y. Wang, A. Kreisel, P. J. Hirschfeld, and V. Mishra, Phys. Rev. B **87**, 094504 (2013).

[34] R. T. Gordon, C. Martin, H. Kim, N. Ni, M. A. Tanatar, J. Schmalian, I. I. Mazin, S. L. Bud'ko, P. C. Canfield, and R. Prozorov, Phys. Rev. B **79**, 100506 (2009).

[35] H. Kim, R. T. Gordon, M. A. Tanatar, J. Hua, U. Welp, W. K. Kwok, N. Ni, S. L. Bud'ko, P. C. Canfield, A. B. Vorontsov, and R. Prozorov, Phys. Rev. B **82**, 060518 (2010).

[36] N. W. Salovich, Hyunsoo Kim, Ajay K. Ghosh, R. W. Giannetta, W. Kwok, U. Welp, B. Shen, S. Zhu, H.-H. Wen, M. A. Tanatar, and R. Prozorov, Phys. Rev. B **87**, 180502 (2013).

[37] Marcin Konczykowski (private communication).

[38] Cornelis Jacominus Van Der Beek, Sultan Demirdis, Dorothée Colson, F. Rullier-Albenque, Yanina Fasano, Takasada Shibauchi, Yuji Matsuda, Shigeru Kasahara, Piotr Gierlowski, and Marcin Konczykowski, arXiv:1209.3586.

[39] S. Yeninas, M. A. Tanatar, J. Murphy, C. P. Strehlow, O. E. Ayala-Valenzuela, R. D. McDonald, U. Welp, W. K. Kwok, T. Kobayashi, S. Miyasaka, S. Tajima, and R. Prozorov, Phys. Rev. B **87**, 094503 (2013).

[40] Yong Liu, M. A. Tanatar, V. G. Kogan, Hyunsoo Kim, T. A. Lograsso, and R. Prozorov, Phys. Rev. B **87**, 134513 (2013).

[41] N. Ni, M. E. Tillman, J.-Q. Yan, A. Kracher, S. T. Hannahs, S. L. Bud'ko, and P. C. Canfield, Phys. Rev. B **78**, 214515 (2008).

[42] R. Prozorov and R. W. Giannetta, Supercond. Sci. Technol. **19**, R41 (2006).

[43] R. Prozorov, R. W. Giannetta, A. Carrington, and F. M. Araujo-Moreira, Phys. Rev. B **62**, 115 (2000).

[44] H. Kim, N. H. Sung, B. K. Cho, M. A. Tanatar, and R. Prozorov, Phys. Rev. B **87**, 094515 (2013).

[45] M. A. Tanatar, N. Ni, S. L. Bud'ko, P. C. Canfield, and R. Prozorov, Supercond. Sci. Technol. **23**, 054002 (2010).

[46] M. A. Tanatar, R. Prozorov, N. Ni, S. L. Bud'ko, and P. C. Canfield, U. S. Patent, 8, 450, 246.

[47] M. A. Tanatar, N. Ni, C. Martin, R. T. Gordon, H. Kim, V. G. Kogan, G. D. Samolyuk, S. L. Bud'ko, P. C. Canfield, and R. Prozorov, Phys. Rev. B **79**, 094507 (2009).

[48] J. Murphy, M. A. Tanatar, D. Graf, J. S. Brooks, S. L. Bud'ko, P. C. Canfield, V. G. Kogan, and R. Prozorov, Phys. Rev. B **87**, 094505 (2013).

[49] M. A. Tanatar, N. Ni, A. Thaler, S. L. Bud'ko, P. C. Canfield, and R. Prozorov, Phys. Rev. B **82**, 134528 (2010).

[50] R. Prozorov, M. A. Tanatar, B. Roy, N. Ni, S. L. Bud'ko, P. C. Canfield, J. Hua, U. Welp, and W. K. Kwok, Phys. Rev. B **81**, 094509 (2010).

[51] K. Cho, H. Kim, M. A. Tanatar, Y. J. Song, Y. S. Kwon, W. A. Coniglio, C. C. Agosta, A. Gurevich, and R. Prozorov, Phys. Rev. B **83**, 060502 (2011).

[52] J. Murphy, C. P. Strehlow, K. Cho, M. A. Tanatar, N. Salovich, R. W. Giannetta, T. Kobayashi, S. Miyasaka, S. Tajima, and R. Prozorov, Phys. Rev. B **87**, 140505 (2013).

[53] N. R. Werthamer, E. Helfand, and P. C. Hohenberg, Phys. Rev. **147**, 295 (1966).

[54] A. M. Clogston, Phys. Rev. Lett. **9**, 266 (1962); B. S. Chandrasekhar, Appl. Phys. Lett. **1**, 7 (1962).

[55] V. G. Kogan and R. Prozorov, Rep. Prog. Phys. **75**, 114502 (2012).

[56] K. Cho, M. A. Tanatar, N. Spyrison, H. Kim, Y. Song, Pengcheng Dai, C. L. Zhang, and R. Prozorov, Phys. Rev. B **86**, 020508 (2012).

[57] S. L. Bud'ko, N. Ni, and P. C. Canfield, Phys. Rev. B **79**, 220516 (2009).

[58] R. Prozorov and V. G. Kogan, Rep. Prog. Phys. **74**, 124505 (2011).

[59] Peter J. Hirschfeld and Nigel Goldenfeld, Phys. Rev. B **48**, 4219 (1993).

[60] R. T. Gordon, N. Ni, C. Martin, M. A. Tanatar, M. D. Vannette, H. Kim, G. D. Samolyuk, J. Schmalian, S. Nandi, A. Kreyssig, A. I. Goldman, J. Q. Yan, S. L. Bud'ko, P. C. Canfield, and R. Prozorov, Phys. Rev. Lett. **102**, 127004 (2009).